CoA Note 133

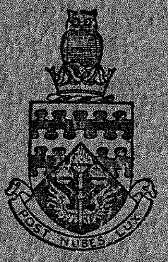

THE COLLEGE OF AERONAUTICS
CRANFIELD

SOME TESTS ON A CIRCULAR GROUND EFFECT MACHINE WITH FORWARD SPEED

by

T. M. Harris, J. H. Davies, and A. J. Alexander

NOTE NO. 133

October, 1962

THE COLLEGE OF AERONAUTICS

CRANFIELD

Some Tests on a Circular Ground Effect Machine with Forward Speed

- by -

*T. M. Harris, D.C.Ae., J. H. Davies, D.C.Ae.,
and A. J. Alexander, M.Sc., Ph.D., A.F.R.Ae.S.

SUMMARY

Wind tunnel tests have been made on a circular wing with 90° downward peripheral blowing both in and out of ground effect. Tests made with two slot widths, a range of blowing pressures and choked jets, indicate that C_μ is a unifying parameter for this type of test. The windspeed was varied between 0 to 200 ft/sec. at zero incidence and the static pressure distribution on both top and bottom surfaces was measured. The sum of the integrated pressures on both upper and lower surfaces agreed reasonably well with the measured overall lift. Flow visualisation on a streamwise plate beneath the model showed the vortex system and the eventual collapse of the forward jet with increasing windspeed.

---

* These tests were made by the first two authors as part requirement for the Diploma of the College of Aeronautics. The work was supervised by Mr. G. M. Lilley and the third author.

CONTENTS

LIST OF SYMBOLS

α	Geometric incidence
V	Free stream velocity
m_j	Rate of mass flow slugs/sec.
v_j	Final jet velocity assuming isentropic expansion to free stream pressure.
L	Measured overall lift
h	Height of flap trailing edge above ground plate at pivot point ($0.5\ c_o$)
D	Diameter of model = 12 in.
p_D	Static pressure of blowing air inside model
p_o	Atmospheric pressure
δ	Slot width in.
L/m_jv_j	Lift augmentation factor = $\frac{\text{Total lift}}{m_jv_j}$
L_u/m_jv_j	$\frac{\text{Upper surface pressure lift}}{m_j\ v_j}$
L_ℓ/m_jv_j	$\frac{\text{Lower surface pressure lift}}{m_j\ v_j}$
T_a/m_jv_j	Non-dimensional apparent jet thrust = $(L - L_u - L_\ell)/m_jv_j$
S	Wing area .785 sq.ft.

1. Introduction

Since the introduction of the ground effect principle a large number of machines embodying this principle have been constructed with varying degrees of success. Theoretical and controlled experimental work however, have lagged far behind and even today with commercial hovercraft under construction there is still no adequate theory and very little published experimental data.

A considerable part of the experimental work has been concentrated on hovering tests and it may be said that this end of the flight regime is fairly well understood. With the high speeds now possible, research into upper surface lift and cushion breakdown are of vital importance and it is hoped that theory and experiment will be able to keep abreast of technical development and not lag so far behind as in the past.

The present tests, made in 1959, used a thin high velocity jet to simplify the distribution problem in the model and the vertical jet path was chosen for simplicity. However, despite the unrepresentative jet arrangement the qualitative behaviour of the model with change in windspeed would appear to be relevant to more practical G.E.M.'s in the light of an almost total lack of published information.

2. Model and Experimental Method

The model used in these tests had a circular planform 1ft in diameter with an elliptic upper surface cross section. The model was made in two halves, the bottom half having a 90° deflected flap at its periphery and forming a peripheral slot when joined to the top half (see Figs. 1 and 2). The jet was turned vertically downwards by means of Coanda Effect. Jet width could be varied by placing shims between the two halves of the model and slot widths of .008 and .014 in. were tested. The model was constructed in steel. Static pressure tappings on top and bottom surfaces are shown in Fig. 2.

High pressure air was fed to the model via a circular ring main designed to give low balance constraints, see Fig. 3. The rate of mass flow of air to the model, m_j, was measured with sharp edged orifice plates and the jet velocity, v_j, was calculated on the assumption that the jet expanded isentropically from the measured plenum chamber pressure in the model to atmospheric pressure. The ideal jet thrust, J, has been taken as $m_j v_j$. The true thrust will be less than J due to the fact that appreciable losses occur in turning the jet through 90° (Wood, 1962).

The tests were made in the College of Aeronautics 8ft x 6ft low speed wind tunnel at speeds ranging from 0 to 200 ft/sec. The ground was represented by a large wooden plate eight feel square and two inches thick stiffened by "L" shaped steel supports to ensure flatness. This ground plate had an elliptic leading edge and a chamfered trailing edge and was set at zero incidence relative to the tunnel stream. A system of screw jacks was used to position the plate vertically.

3. Discussion of results

Static tests, in which the overall lift was measured, were performed at zero incidence with two slot widths .008 in. and .014 in. at blowing pressure ratios of 5.83 and 3.90. The variation of the non-dimensional lift, $\left(\frac{\text{Lift}}{m_j v_j}\right)$, with h/D, is given in Fig. 4 and it is seen that very nearly the results fall on to a single curve.

The effect of forward speed on lift augmentation is shown in Figs. 5 - 8. $\frac{L}{m_j v_j}$ is the total lift augmentation, as calculated from the balance measurements, $L_u/m_j v_j$ and $L_\ell/m_j v_j$ are the integrated pressure lift augmentations on the upper and lower surfaces respectively and $T_a/m_j v_j$ is the non-dimensional apparent jet thrust defined as $(L - L_u - L_\ell)/m_j v_j$. This definition takes into account the jet turning losses due to ground proximity and forward speed.

With increasing forward speed the upper surface of the model produces aerodynamic lift due to the camber effect and at relatively low speeds the lower surface lift is unchanged from its value at zero forward speed. At a certain critical speed, however, depending on height and planform, the dynamic head of the oncoming stream exceeds the cushion pressure sufficiently to bend the forward jet sheet back under the model. The resulting suction near the nose on the lower surface, see Fig. 11, causes a drop in the undersurface and total lift near the critical speed. Above this speed the increasing upper surface lift more than compensates for the reduced lower surface lift. Close to the ground, h/D = .083, Fig. 5, the critical speed is about 200 ft/sec and the total lift is relatively unaffected up to this windspeed. The apparent jet thrust ratio $T_a/m_j v_j$ is very low even for the static case $\left(\frac{T_a}{m_j v_j} = 0.67\right)$ and decreases slightly with forward speed. Figs. 6 - 8 show comparable results for h/D ratios of 0.25, 0.417 and ∞ (no ground board). The change in lift, for h/D =0.417, around the critical speed, which at this height ratio is 100 ft/sec, can be clearly seen in Fig. 7. In all cases T_a decreases from its static value with increasing windspeed and also with decreasing h/D, Fig. 9. The wind on results of the pressure measurements are considered less reliable than wind off as the number of pressure holes on the top surface are few and do not cover the important region near the slot; but it is significant that the same trend is observed at all windspeeds.

The results shown in Figs. 5 - 8 are for one pressure ratio, $p_D/p_o = 4.38$. However, balance measurements only were taken at pressure ratios of 2.45, 2.93, 3.41, 4.38 for windspeeds up to 215 ft/sec. and the results are shown in Fig. 10 where values of $L/m_j v_j$ are plotted against C_μ. At the smallest ground clearance, h/D = 0.083, agreement between the results at the three lowest pressure ratios is good but does not show the critical speed clearly. For h/D = 0.25 and 0.417 the critical speed is shown clearly with the results for various pressure ratios showing good correlation. The nature of the breakdown is also shown, and is more severe at lower ground clearances. Stars indicate the estimated critical C_μ from flow visualisation tests.

Fig. 11 shows the effect on the lower surface pressures (along wind) of increasing windspeed at h/D = 0.417. At zero windspeed the pressure distribution along wind is symmetrical and is little changed at 50 ft/sec. At 100 ft/sec., where flow visualisation showed the forward jets to be deflected backwards, large suction pressures occur near the nose and increase with further increase in windspeed.

A plate was inserted vertically between the model and ground plate along wind and a mixture of Alabastine, Teepol and water applied to visualise the flow.

Tunnel speed and jet velocity were then quickly increased to the appropriate values and the mixture allowed to dry. Figs. 12a and 12b show the change in flow pattern under the model with increase in wind speed at a constant height h/D =0.417 incidence and jet velocity. In this case the critical speed is about 80 ft/sec.

Fig. 13 shows the effect on lower surface pressures along the model centre line of change of incidence at zero tunnel speed for h/D = 0.25 and the large suction pressure induced on the lower edge due to the chordwise flow which give rise to unstable pitching moments.

4. Reference

1. Wood, M.N. Comparative thrust measurements on a series of jet-flap configurations and circular nozzles. R.A.E. T.N. Aero.2804. 1962.

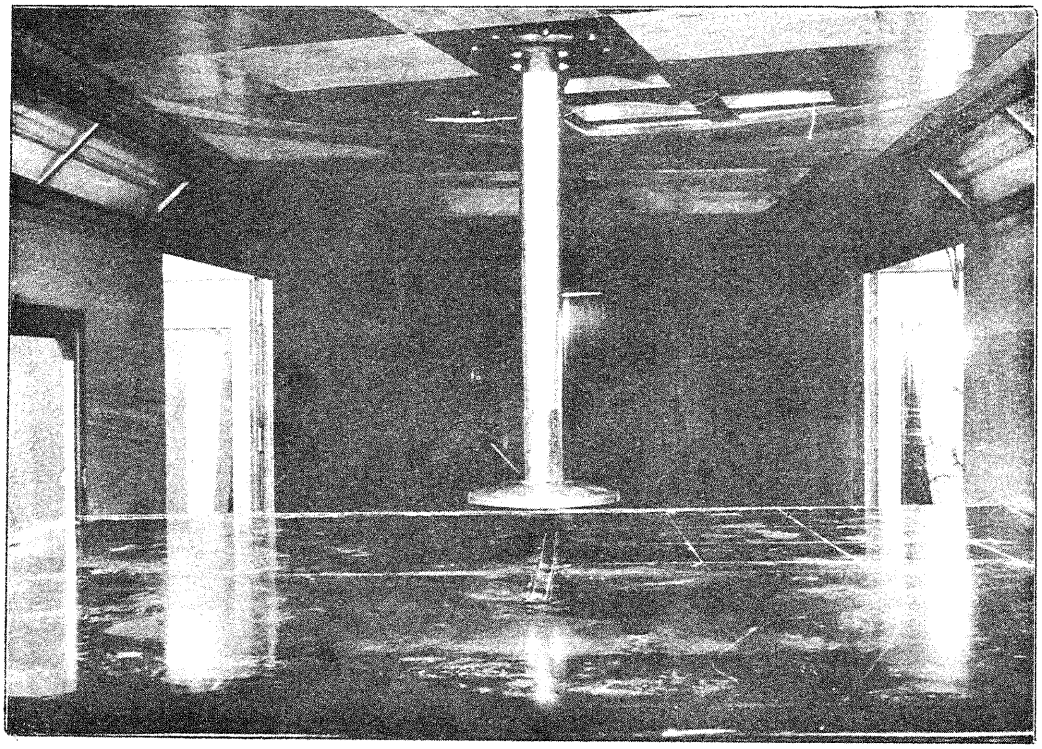

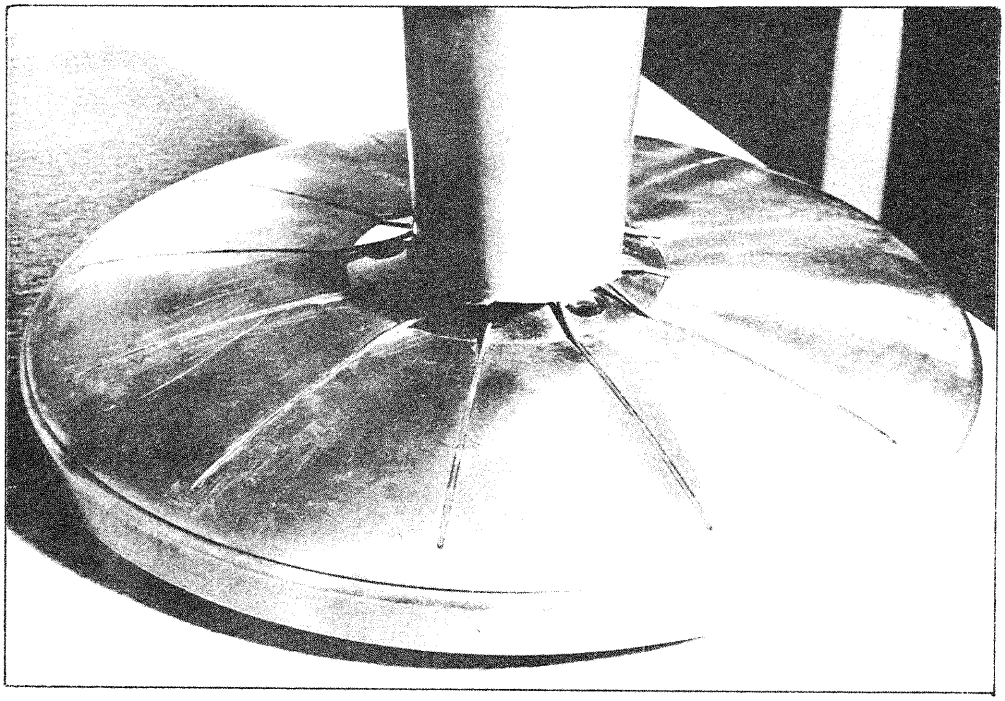

FIG. 1. THE MODEL

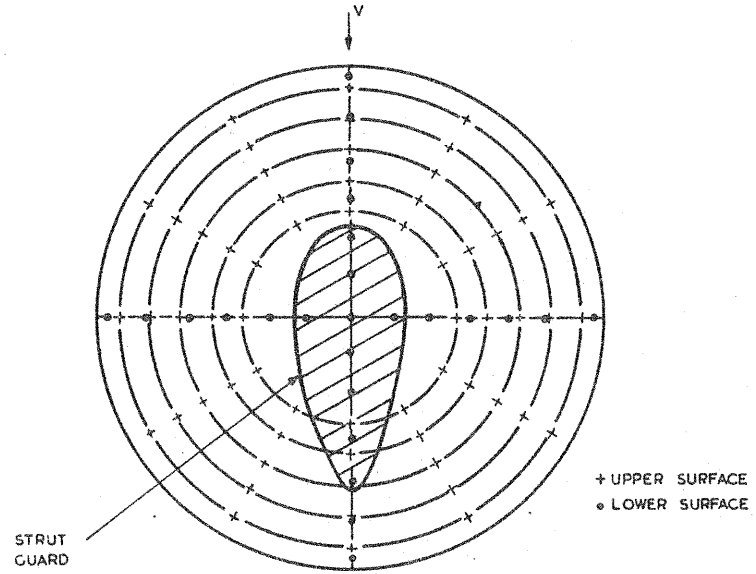

FIG. 2a POSITIONS OF SURFACE STATIC PRESSURE HOLES

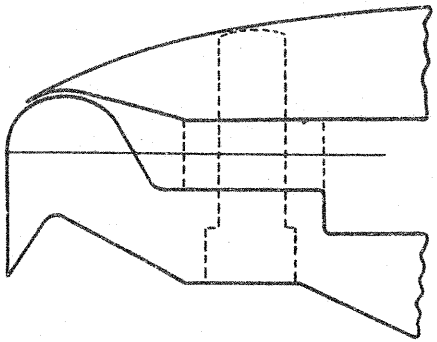

FIG. 2b BLOWING SLOT

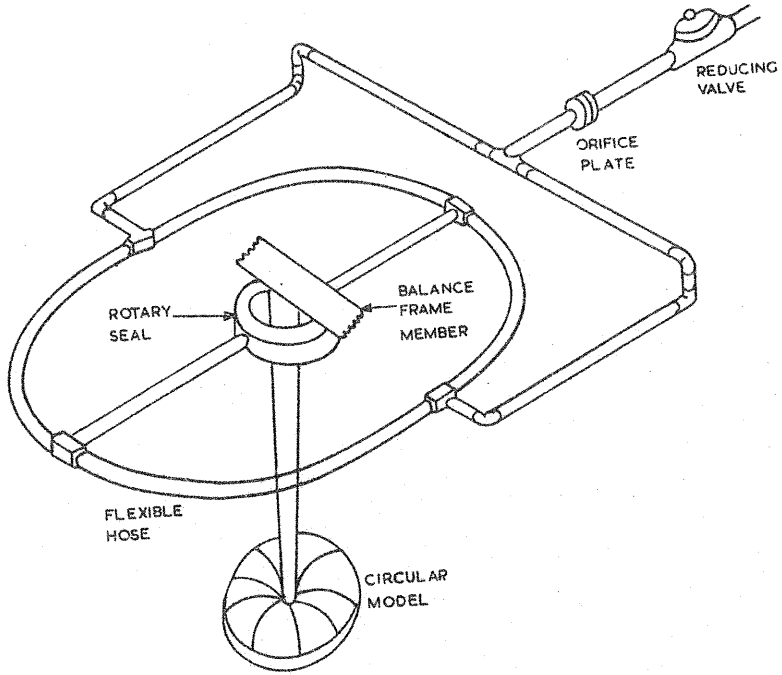

FIG. 3. MODEL MOUNTING

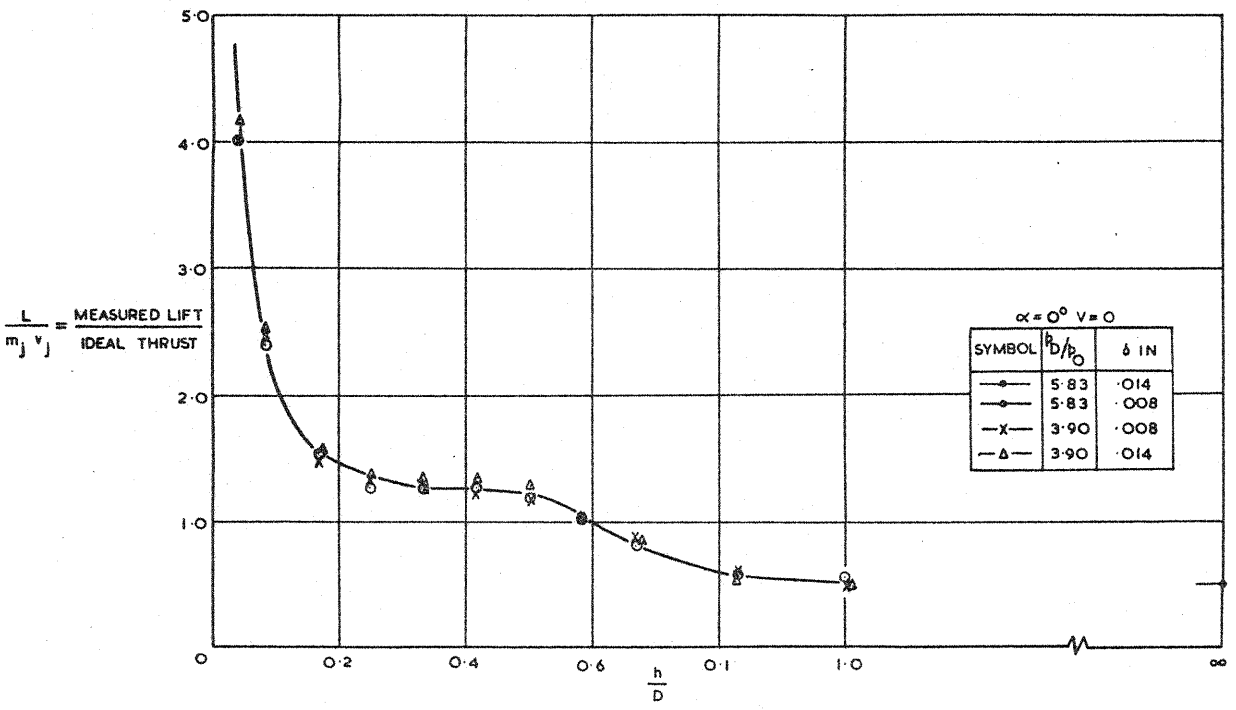

FIG. 4. VARIATION OF LIFT AUGMENTATION WITH HEIGHT

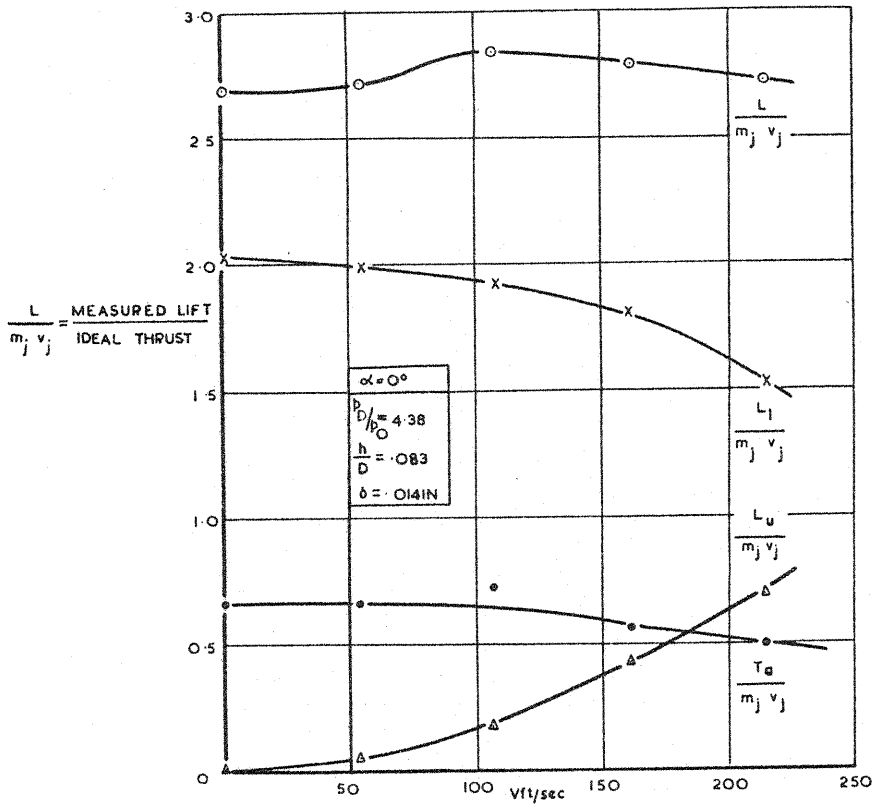

FIG. 5. VARIATION OF LIFT AUGMENTATION WITH WINDSPEED h/D = .083

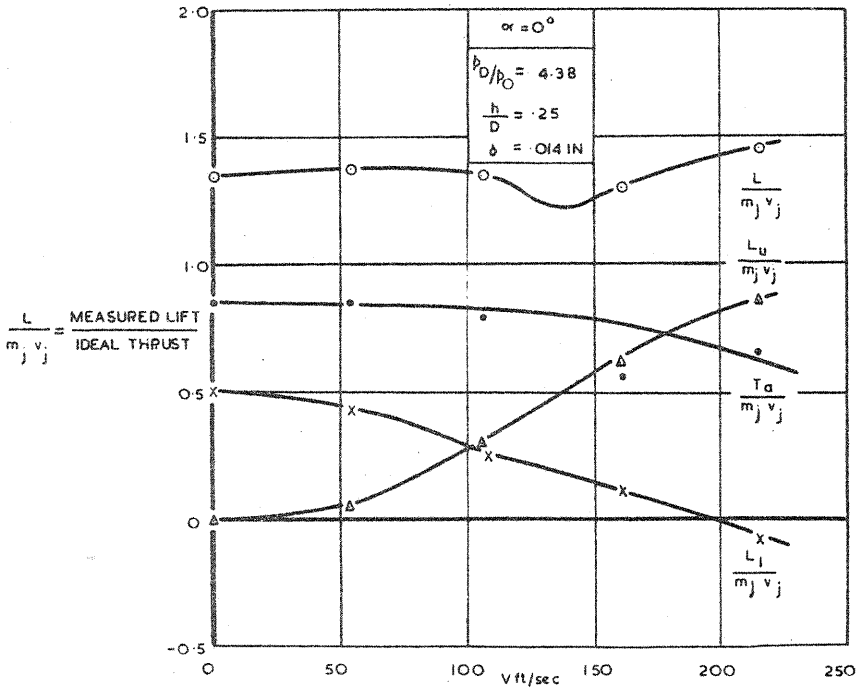

FIG. 6. VARIATION OF LIFT AUGMENTATION WITH WINDSPEED h/D = .25

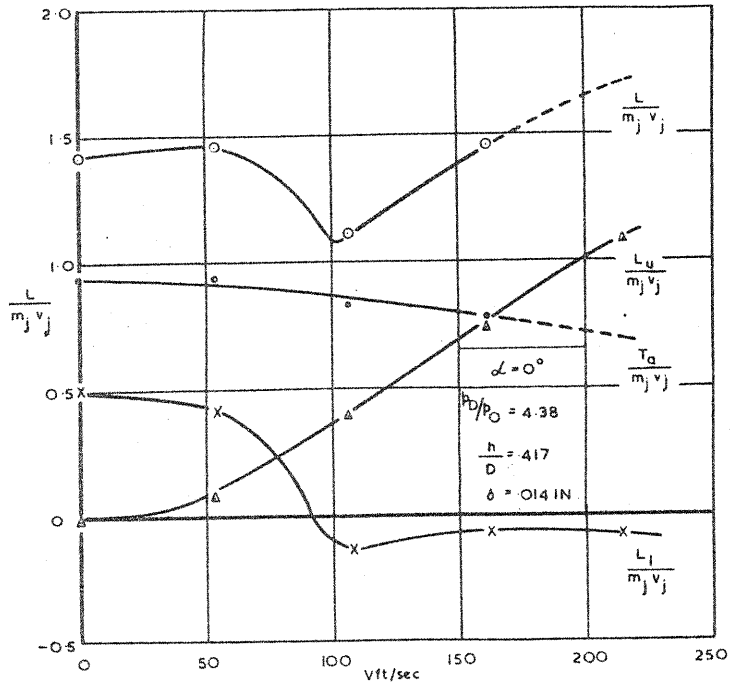

FIG. 7. VARIATION OF LIFT AUGMENTATION WITH WINDSPEED h/D = .417

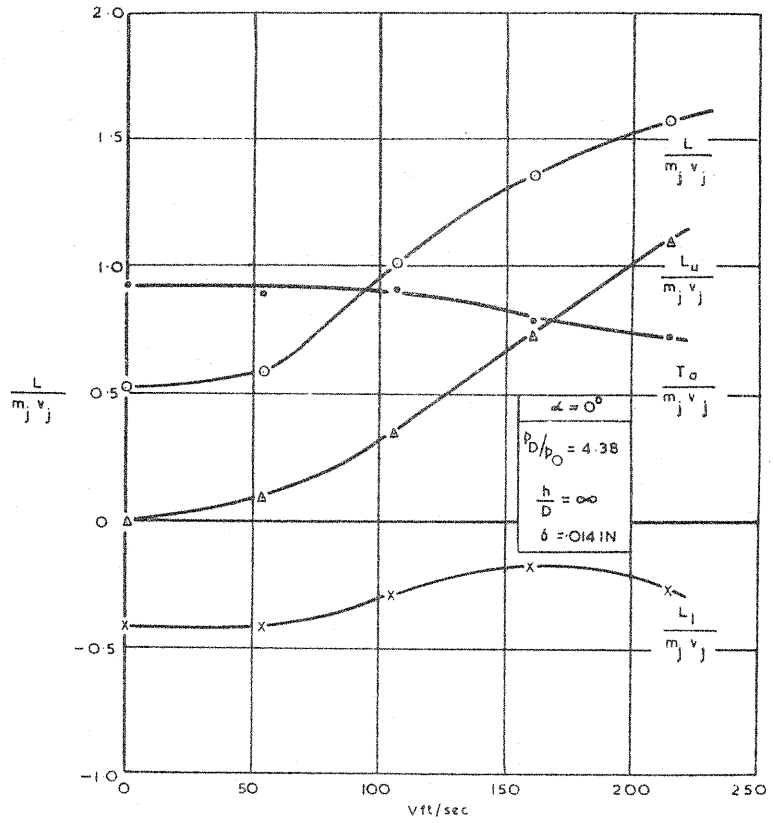

FIG. 8. VARIATION OF LIFT AUGMENTATION WITH WINDSPEED h/D = ∞

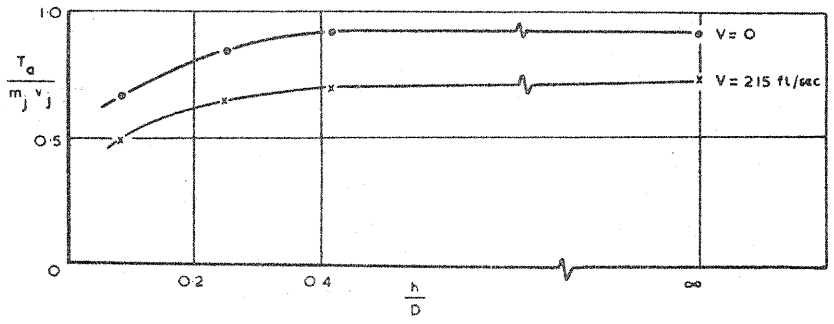

FIG. 9. VARIATION OF JET THRUST WITH HEIGHT AND WINDSPEED $\alpha = 0^{\circ}$ $P_D/P_o = 4.38$

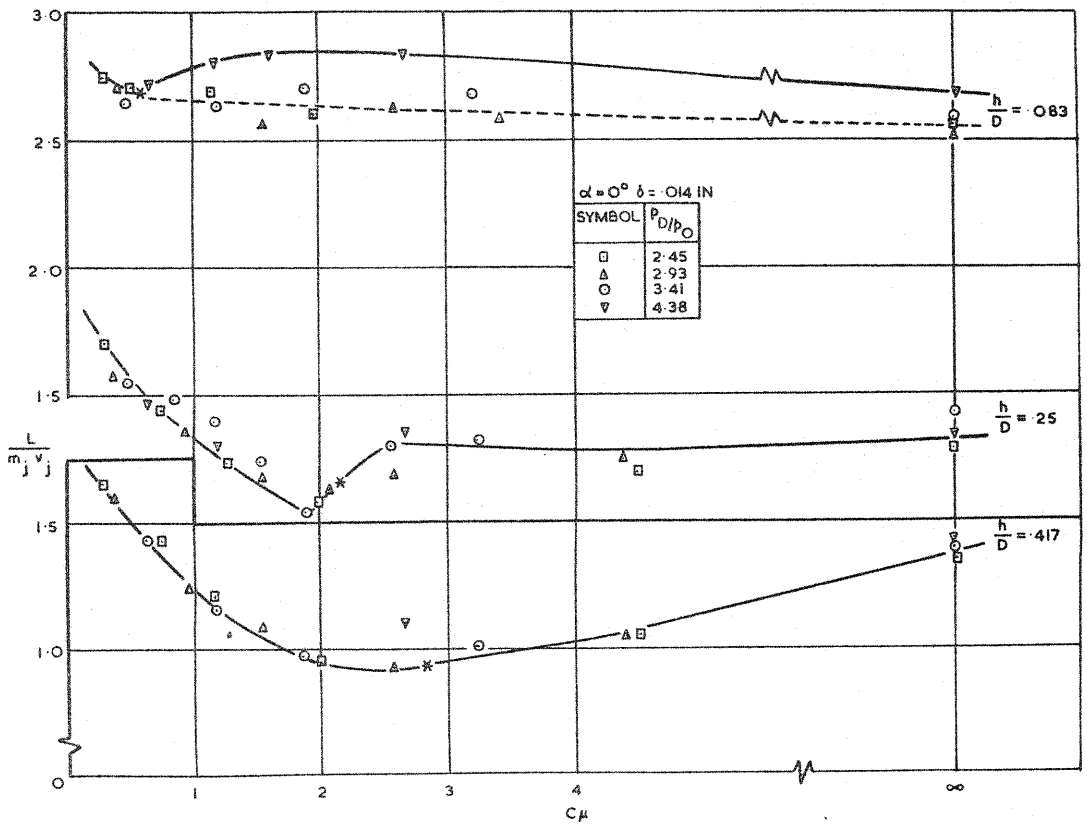

FIG. 10. VARIATION OF LIFT AUGMENTATION WITH MOMENTUM COEFFICIENT

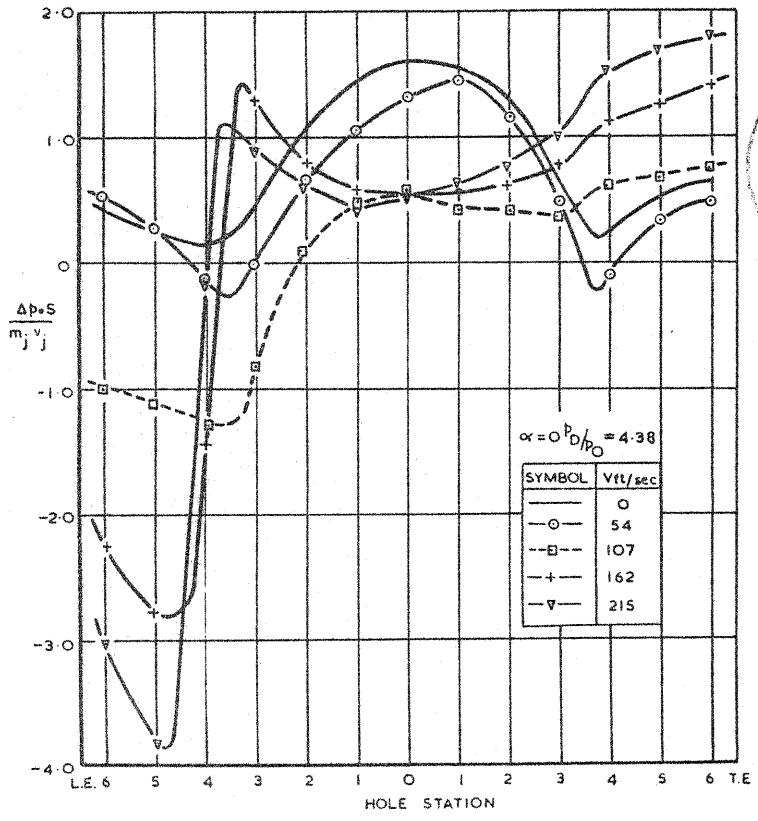

FIG. 11. VARIATION OF LOWER SURFACE STATIC PRESSURES WITH WINDSPEED h/D = ·417

V = 0

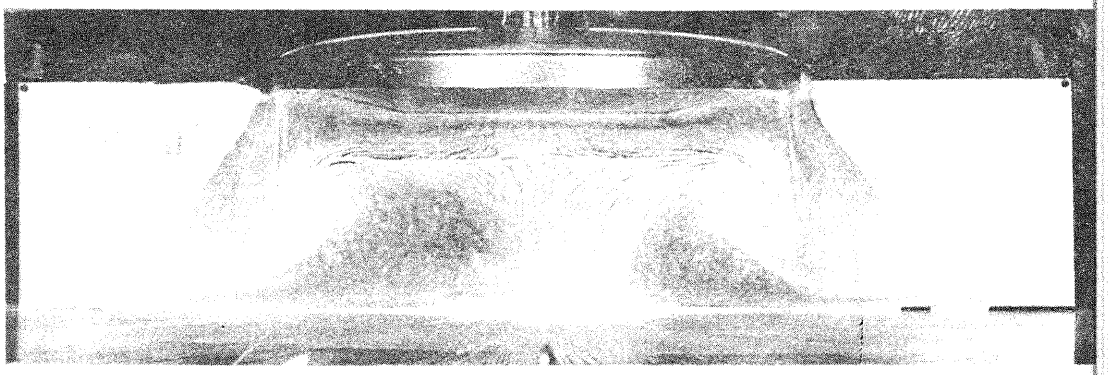

V = 50 fps

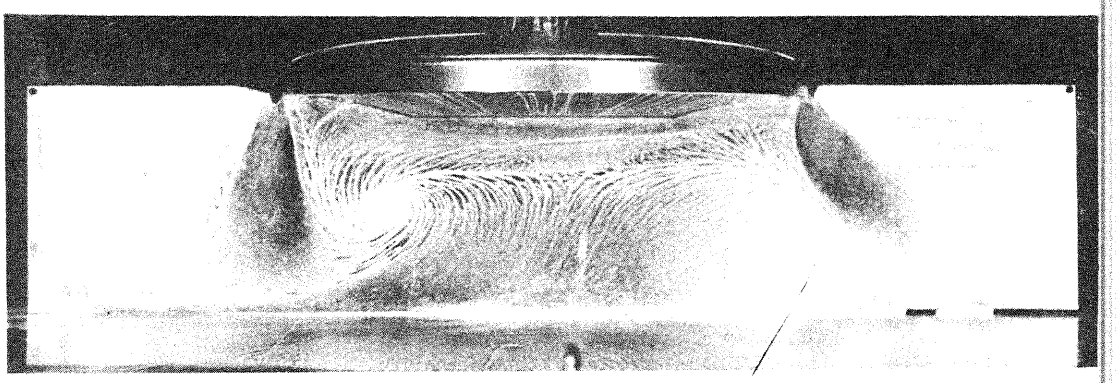

V = 75 fps

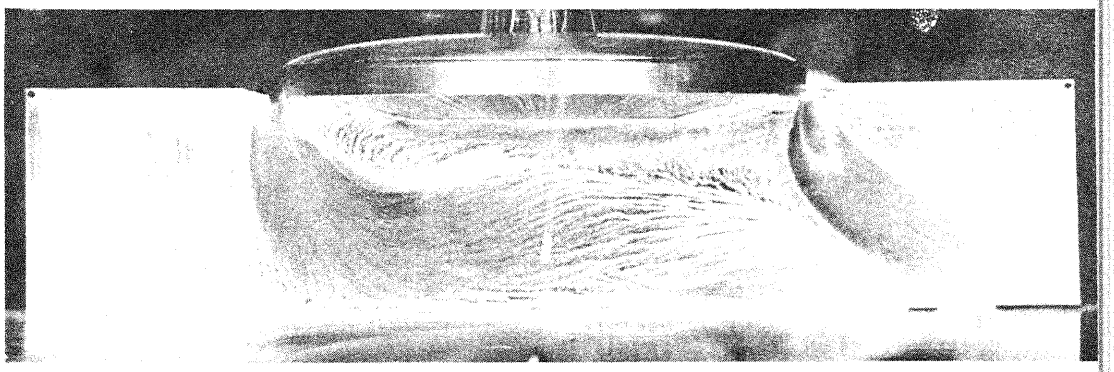

V = 80 fps

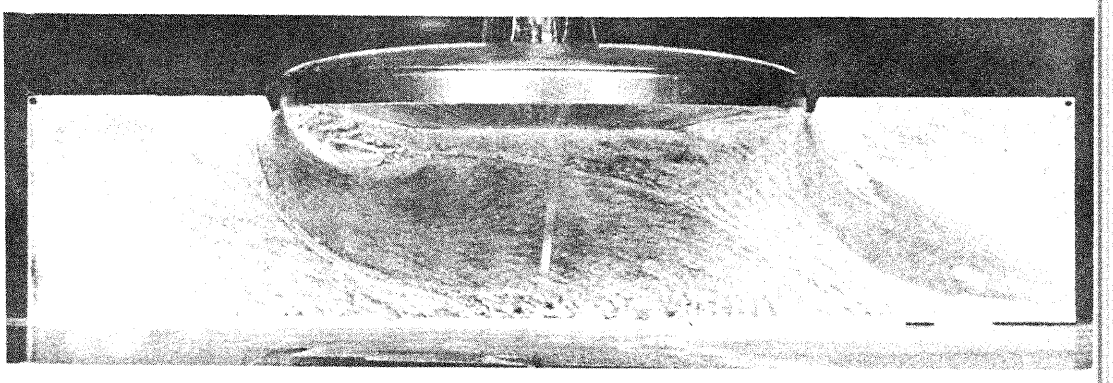

FIG. 12a FLOW VISUALISATION ON A STREAMWISE PLATE α = 0, h/D = .417, p_D/p_o = 3.90

V = 100 fps

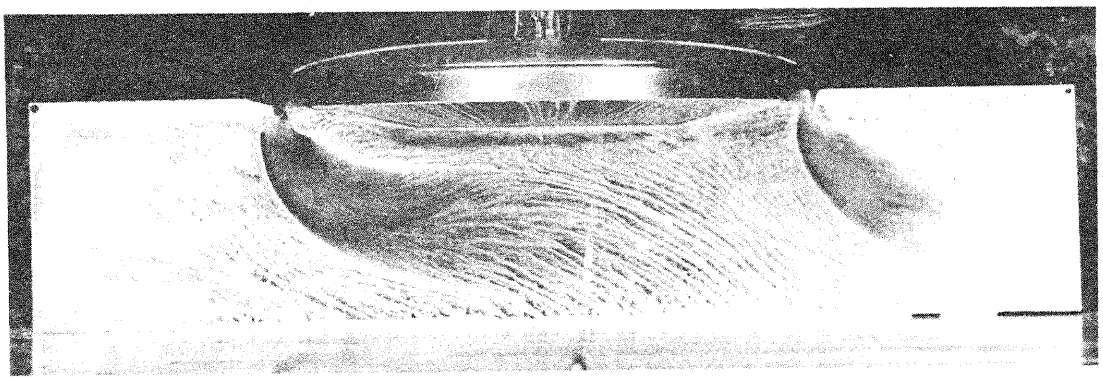

V = 125 fps

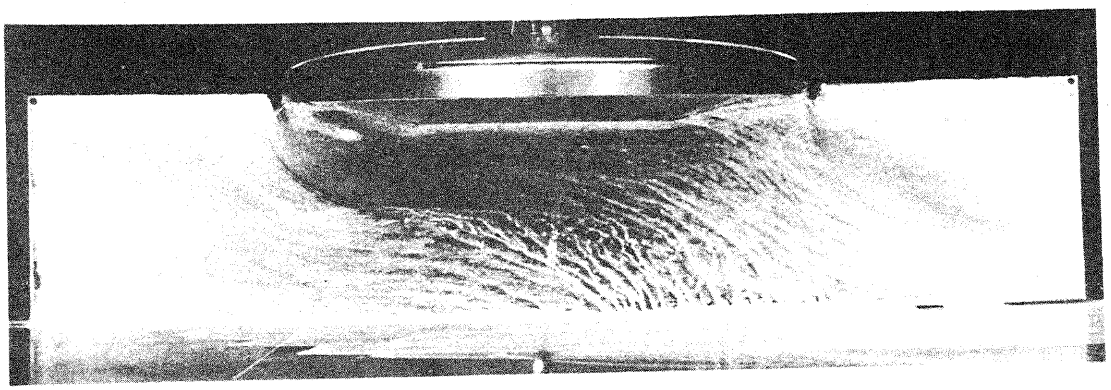

V = 150 fps

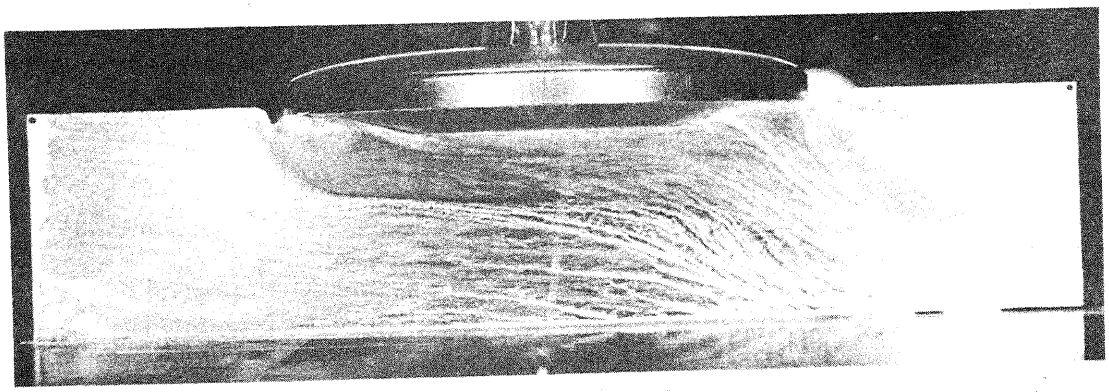

V = 200 fps

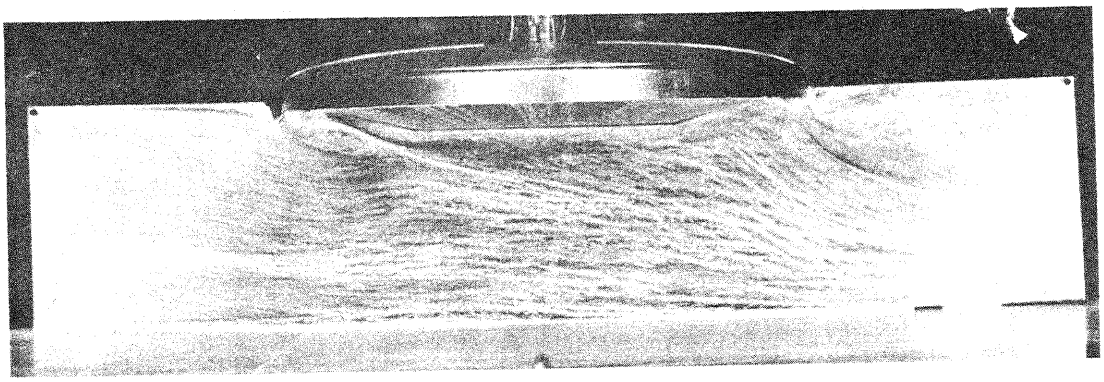

FIG. 12b FLOW VISUALISATION ON A STREAMWISE PLATE α = 0, h/D = .417, p_D/p_o = 3.90

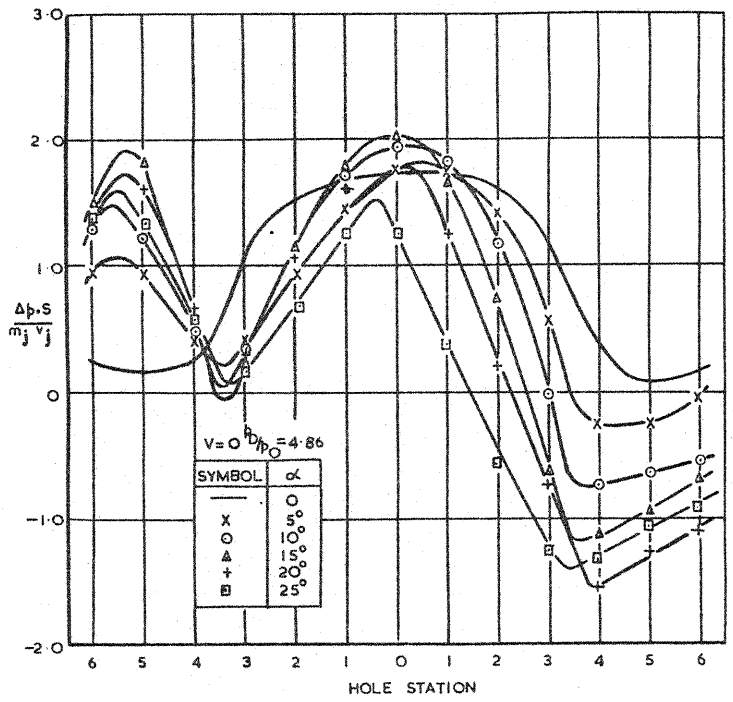

FIG. 13. VARIATION OF LOWER SURFACE STATIC PRESSURES WITH INCIDENCE h/D = .25